J. exp. Biol. **170**, 1–18 (1992)
Printed in Great Britain © *The Company of Biologists Limited 1992*

STRENUOUS EXERCISE-INDUCED REMODELLING OF MATURE BONE: RELATIONSHIPS BETWEEN *IN VIVO* STRAINS AND BONE MECHANICS

BY BARBARA J. LOITZ AND RONALD F. ZERNICKE
Department of Surgery, University of Calgary, Calgary, AB T2N 4N1, Canada

Accepted 11 May 1992

Summary

Mature bone can adapt to strenuous exercise, but no study has correlated the changes in bone *in vivo* strains, remodelling and mechanical properties that occur as a consequence of strenuous training. Therefore, we examined exercise-related remodelling and *in vivo* strains in the tarsometatarsus (TMT) of three groups of adult (post-physial closure) White Leghorn roosters: basal control (30 weeks of age), age-matched control (39 weeks) and exercise (39 weeks). Exercise birds ran for 1 h a day, 5 days a week for 9 weeks at 70–75 % of predicted maximum aerobic capacity. During treadmill locomotion, *in vivo* strains were recorded from miniature rosette strain gauges implanted on anterior, medial and lateral TMT cortices. TMT mechanical properties were measured with three-point bending tests to failure. Cortical morphometry was digitized from photographic slides of a 1-mm thick mid-diaphysial cross section of each bone. Exercise and age-matched control TMTs had significantly greater cortical area and maximum load than had basal controls. Exercise axial strains significantly exceeded basal and age-matched control strains along the anterior and lateral surfaces. Age-matched control anterior axial strain was twice that of the basal control. The mature bone remodelling suggested that the structural properties optimized by exercise-induced remodelling may differ from those optimized by age-related remodelling. The findings support the osteoregulatory role of strain but contradict earlier data suggesting that strain magnitudes do not change significantly with age or exercise.

Introduction

Bone appears to be sensitive to dynamic strains, but the nature of the mechanical stimulus producing remodelling is poorly understood, and the specific structural properties optimized during remodelling remain unclear (Cowin *et al.* 1984). Rubin (1984) states that bone structure is a balance of form and mass requirements for strength – within the constraints of tissue metabolic economy. Currey (1984) and Currey and Alexander (1985) hypothesize that bone remodels to optimize mechanical properties while minimizing the mass of a biological

Key words: biomechanics, bone strain, remodelling, strenuous exercise, chicken.

system. The structural loading that can occur in limb bones during periods of strenuous activity provides a means to test the verity of the Currey–Alexander hypothesis, because during endurance exercise both mass minimization (energy conservation) and bone mechanical properties may have potent effects on the remodelling of bone.

Here, we examined exercise-related adaptations of adult (post-physial closure) bone, because with immature animals the effects of growth- and exercise-related remodelling are intertwined, and the generalization that exercise benefits immature bone remains equivocal. For example, short-term (9 weeks) strenuous exercise retarded the normal increase in avian tarsometatarsus length and flexural rigidity (Matsuda *et al.* 1986), and mouse femur longitudinal growth was retarded following 3–12 weeks of intense exercise (Kiiskinen, 1977), but 1 year of moderate exercise increased the strength and energy absorption of immature swine femur (Woo *et al.* 1981). In adults, however, regular endurance exercise is reported to be generally advantageous; with exercise, loadbearing bones increase in cortical thickness (Jones *et al.* 1977), mineral content (Krolner *et al.* 1983) and mass (Dalen and Olsson, 1974; Pirnay *et al.* 1987).

To examine the local strain milieu of a loadbearing bone during exercise, we quantified *in vivo* strains and mechanical and geometrical properties of the tarsometatarsus (TMT) of adult roosters. Baseline measures of bone strain, mechanics and morphology were gathered from a basal control group at the start of the 9-week experiment and a sedentary control group (age-matched to the exercise group) provided data to reveal remodelling specifically related to age differences (30-week-old basal group *vs* 39-week-old age-matched control group). Roosters in the exercise group ran strenuously (70–75 % maximum aerobic capacity) for 9 weeks and, consistent with the Currey–Alexander hypothesis, the TMT ultimate or impact strength appeared to be maximized with a conserved bone mass.

Materials and methods

Animals

Skeletally mature (post-physial closure; 30 weeks) White Leghorn roosters (UCLA Vivarium) were divided randomly into three groups: basal control (N=9 roosters), sedentary age-matched control (N=11) and exercise (N=12). Long bone physes of White Leghorn roosters close at 20 weeks (Latimer, 1927). Each of these three groups was divided into three subgroups: no surgery (N=4–7), surgery with strain-gauge implantation and recording (N=3) and sham surgery (N=2). Bone morphology and mechanics and gait kinematics were measured for all 32 roosters. The sham-surgery subgroup tested whether the surgery itself altered gait, after the 48-h post-surgery recovery. All roosters were housed in outdoor, covered runs (1.5 m×6.5 m×2.0 m; 8 roosters per run; natural light:dark cycle; average temperature 13–35 °C) with *ad libitum* access to food and water.

All basal control roosters were killed (CO_2 asphyxiation) within 14 days after

the beginning of the experiment. Sedentary age-matched control roosters had *ad libitum* activity in the caged runs, but received no treadmill exercise training. Age-matched control and exercised animals were killed at the end of the experiment (39 weeks of age).

During the 9 week duration of the experiment, exercised roosters ran (5 days per week) in individual lanes (15 cm×48 cm×25 cm) on a custom-made motorized treadmill. The exercise protocol started with 1 week of progressive exercise, so that the animals were able to run continuously for 1 h by the end of the first week. For the remaining 8 weeks, animals ran 1 h per day, 5 days per week at an exercise intensity of approximately 70–75 % of maximum aerobic capacity – as predicted by the linear relationship between treadmill running speed and oxygen uptake in domestic fowl (Brackenbury and Avery, 1980). As the roosters' aerobic capacity improved with training, running speed was increased to maintain the same relative physiological intensity. After 9 weeks, the sedentary age-matched control and exercise roosters were assigned randomly to one of three subgroups: no surgery, sham surgery or surgery with strain-gauge implantation. All experimental procedures were approved by the UCLA Chancellor's Animal Research Committee (protocol no. 88–176) and conformed to policies and procedures stated in *Laboratory Animals in Teaching and Research* and the provisions of the *NIH Guide for the Care and Use of Laboratory Animals.*

Strain gauge instrumentation

Constantan–foil electrical-resistance (120 Ω), delta-rosette strain gauges (EA-06-030YB-120, Measurements Group Inc, Raleigh, NC) were used. Overall gauge dimension was 2.64 mm×5.08 mm, with the superior and inferior planar elements placed 60° with respect to the transverse element. Stranded silver-coated copper wire (CZ 1174SPC, Cooner Wire, Chatsworth, CA; 36 gauge, 45 cm long) leads were soldered to tabs on each gauge and waterproofing silicone (RTV 16, E.V. Roberts Co., Culver City, CA) was applied to the elements, solder tabs and lead wires. The silicone cured 48 h prior to gauge implantation. Immediately prior to data recording, male connector pins (Amphenol no. 220-PO2-100, Newark Electronics, Inglewood, CA) were soldered to each element lead for connection to a lead (24 gauge) coming from the bridge amplifier.

During *in vivo* tests, strain gauges were employed in a Wheatstone quarter bridge with a 0.22-V excitation from a d.c. current source (model 7P1D, Grass Instrument Co., Quincy, MA). Bridge amplifiers interfaced directly with an IBM-AT computer, allowing analog-to-digital data conversion at a sampling rate of 100 Hz with a 12-bit accuracy over ±200 mV. The bridge was balanced *via* computer and custom software (IBM AT, Boca Raton, FL, and Computerscope ISC-16, RC Electronics, Santa Barbara, CA).

Surgical protocol

All surgery was performed on the right tarsometatarsus (TMT) bone. Following anesthesia (intramuscular sodium pentobarbital, 35 mg kg^{-1} body mass) and appli-

cation of a femoral tourniquet, a longitudinal incision was made along the medial aspect of the TMT, beginning approximately 2 cm distal to the ankle joint and stopping 2 cm proximal to the tarsometatarsophalangeal joint. While preserving superficial vasculature, we excised the keratinized skin over the medial, anterior and lateral TMT surfaces. Excision of the skin was necessary because the keratinized nature of the tissue prevented it from being sutured effectively. Sites for gauge implantation were identified, and the periosteum from a 6 mm×8 mm area was removed with a scalpel from each bony site. Exposed cortical surfaces were degreased with alternating cotton-swab applications of alcohol and acetone. Cyanoacrylate cement (Loctite Superbond, E.V. Roberts Co., Culver City, CA) was used to bond prepared strain gauges to the cleaned surfaces; pressure was applied for approximately 1 min to ensure adequate cement curing. An 8 mm×10 mm piece of latex was then bonded with cyanoacrylate to the bone, strain gauge and leads, waterproofing the entire instrumented area. Medial, anterior and lateral rosette gauges were attached and waterproofed separately. Strips of sterile wound dressing (Op-Site, UCLA Medical Storehouse, Los Angeles, CA), sterile gauze and stockinette protected the surgical sites and leads following gauge implantation.

Strain gauge leads were stress-relieved during application of the surgical dressings and passed subcutaneously between an entry site at the distal tibia and an exit site at the dorsal midthoracic spine. Wires were coiled and taped securely between the rooster's wings. An additional surgical stockinette over the entire lower extremity covered all wounds and exposed leads, preventing the bird's access to surgical sites. During a 48-h postoperative period, intramuscular injections of Talwin (1 mg kg^{-1} body mass) were administered every 4–6 h if the bird demonstrated altered movement patterns indicative of pain. Following data recording, 48 h after surgery, animals were killed and TMTs were excised bilaterally. TMTs were immediately wrapped in paper towels soaked in 50 mmol l^{-1} phosphate buffer solution (pH 7.4), hermetically sealed with clear plastic wrap and aluminum foil, and placed in the freezer (−20 °C) until the day of mechanical testing.

Data collection

Strain measurements

With the bird's instrumented leg quiescent and unloaded, each bridge was balanced. Four data channels were recorded during each trial: three elements of one gauge and one anterior gauge element. The same anterior element was recorded for each trial to allow comparisons across trials. *In vivo* strains were recorded over a 20-s sampling period while implanted roosters in each of the three groups (basal, age-matched control and exercise) walked on the treadmill at 37 cm s^{-1}. This speed was chosen because all the roosters, including the sedentary age-matched ones, could walk effectively on the treadmill at 37 cm s^{-1}. This common speed allowed the direct comparison of the bone strains of each of the

three groups. In addition, because the exercise animals were accustomed to and trained at much faster speeds of walking, we recorded both at a *slow* walk ($37\,cm\,s^{-1}$) and at a *fast* walk ($87\,cm\,s^{-1}$) for each strain-gauge-implanted exercise rooster. This allowed us to examine the speed-related differences in TMT strains for the exercised roosters.

Cinematographic data

A motor-driven 16-mm camera (model 1PL, Photosonics, Burbank, CA) operating at $100\,frames\,s^{-1}$ (verified by internal timing lights) filmed each trial to allow quantification of gait characteristics. To synchronize film and strain-gauge data during each test, a neon light sent a pulse to the computer as the light was illuminated in the field of view. Times of toe-off, midstance and midswing were identified bilaterally from the film using a pin-registered projector (model M16-C, Vanguard, Melville, NY), so kinematic events could be correlated with strain-gauge output.

The walking cycle was referenced to the instrumented (right) limb. Right toe-off marked the beginning and end of a stride. Right midstance occurred when the left foot passed the right ankle joint; right midswing occurred when the right foot passed the left ankle. Toe-off was the last frame that the foot was in contact with the treadmill. The temporal events were determined from the film and matched with phases of the gait cycle.

Mechanical testing

On the day of testing, each left TMT was thawed (22°C), and all muscles and soft connective tissues were removed. Bone lengths were measured ($\pm 30\,\mu m$) with a precision caliper (Brown and Sharpe, North Kingstown, RI) from the proximal TMT plateau distally to the articular surface for the second phalanx. Tissues were temperature-equilibrated (37°C) in a buffer solution ($50\,mmol\,l^{-1}$ potassium phosphate buffer, pH 7.4) for at least 1 h prior to testing.

A servocontrolled electromechanical testing system (model 1122, Instron Corporation, Canton, MA) loaded each TMT (posterior-to-anterior direction) in three-point bending until failure (Matsuda *et al.* 1986). Bones were loaded at the mid diaphysis while submerged in the circulating potassium phosphate buffer (37°C). A fixture with an intersupport distance of 45 mm was used for the lower support, with a 3.2 mm radius of curvature used for all contact points. A small tare load applied to the bone prior to testing prevented rotation during loading. All tests were performed at a crosshead speed of $25.4\,cm\,min^{-1}$.

Analog load–time data from the Instron were converted to digital data (IBM AT and Computerscope ISC-16, RC Electronics, Santa Barbara, CA) with 12-bit accuracy sampled at 2 kHz over an input range of 10 V. A custom-designed computer program (Run Technologies, Los Angeles, CA) was used to calculate TMT structural and material properties. Using interactive computer graphics, five events were marked on the load–time curve of each trial: (1) initial load, (2 and 3) boundary points of the linear loading region, (4) proportional limit, and (5) failure

load. All data samples between the second and third marks were used to compute a least-squares regression line. The proportional limit (mark 4) was the first deviation of the load–time curve from the regression line. The accuracy of identifying this event was related to the observer's ability to distinguish the point on the computer screen. Given the resolution of the screen, the variability was less than 2 % of the mean nonlinear displacement or less than 3 % of the mean load at the proportional limit of each group. The computer software detected maximum load.

With the second moment of area about the bending axis (A_x) and the distance from the tensile periosteal surface to the centroid (c), a program calculated the following mechanical parameters: loads and displacements at the proportional limit, and maximum and failure points; tensile stress at the proportional limit; flexural rigidity; and elastic modulus. Tensile stress at the proportional limit was calculated as Mc/A_x, where M is the bending moment at the proportional limit [proportional load x $(p/4)$; where p is intersupport distance]. Flexural rigidity was calculated as: $EA_x=(p^3/48)(dF/dL)$, where dF/dL is the slope of the linear region of the load-displacement curve. Elastic modulus (E) was calculated by dividing flexural rigidity by A_x.

Calculations of bone mechanical properties were made with the following assumptions (Torzilli *et al.* 1981): (1) bone cross-sectional geometry remains constant between outer support points, (2) St Venant's principle is held (stress can be considered similar throughout the structure tested), (3) out-of-plane bending and torsional reactions are negligible, (4) cross-sectional planes remain planar, and (5) crosshead displacement equals midpoint deflection. Cross-sectional geometry was assessed along TMT length and did not differ significantly within 15 mm to each side of the mid-diaphysial section. The hemispheric crosshead probe did not locally indent the mid diaphysis and, thus, the crosshead displacement was the same as the deflection of the mid diaphysis of the TMT.

Morphometry measures

Using a low-speed (130 revs min^{-1}) slotting saw (Unimat 3, EMCO, Columbus, OH), a 1-mm mid-diaphysial cross section was cut from each right TMT. Slides were taken of each section (Ektachrome, 100 ASA, Eastman Kodak, Rochester, NY, Olympus OM2S, 50 mm flat-field lens, f/3.5, Asanuma auto-bellows, Tokyo, Japan) and rear-projected (magnification 12×). Cross sections were traced and digitized (AST Premium/286 computer, AST Research, Irvine, CA, with 50 cm× 60 cm Sigma Scan tablet, Jandel Scientific, Corte Madera, CA). A modified version of SLICE (Nagurka and Hayes, 1980) calculated second moments of area about major and minor bending axes, periosteal and endosteal diameters, cortical areas and regional cortical thicknesses. Mid-diaphysial cortical morphology was also expressed as rad/t, where rad is periosteal radius and t is cortical thickness (Currey and Alexander, 1985).

Mid-diaphysial cross sections were lyophilized for bone density calculations. The mass of each lyophilized section was measured (±0.10 mg), and density

($mg\,ml^{-1}$) was computed using cortical areas obtained from the cross-sectional morphometry.

Strain computations

Power spectral analysis (ANAPAC, RC Electronics, Santa Barbara, CA) of random trials revealed that 95 % of the strain gauge output was at a frequency less than 5 Hz. Thus, strain gauge data were filtered with a low-pass, nonrecursive digital filter (ANAPAC) with a 5 Hz cut-off frequency.

A custom FORTRAN program calculated strain from the filtered gauge output. Strain-gauge output (ΔS), measured as change in voltage, was used to calculate change in gauge resistance (ΔR) and strain (S) using the following equations (Dally and Reilly, 1978):

$$\Delta E = I\,\Delta R$$

and

$$\Delta R/R = fS,$$

where I is circuit current, R is initial gauge resistance, and f is gauge factor, which is 2.08. From each element's orientation (Fig. 1A) and strain output (S), the bone's axial (S_a), transverse (S_t) and shear (G) strains (Fig. 1B) were calculated. Peak strains were averaged from 10 steps for each rooster.

Statistics

Multivariate analysis of variance (SAS, Statistical Analysis System, SAS Institute, Cary, NC) was used to detect significant differences in the morphological and biomechanical variables and in peak strains among the three groups. Ryan–Einot–Gabriel–Welsh multiple range tests (SAS) were used for *post hoc* comparisons to reveal locations of mean differences in significant overall F-tests. Significance was evaluated at $P<0.05$ for all statistical tests.

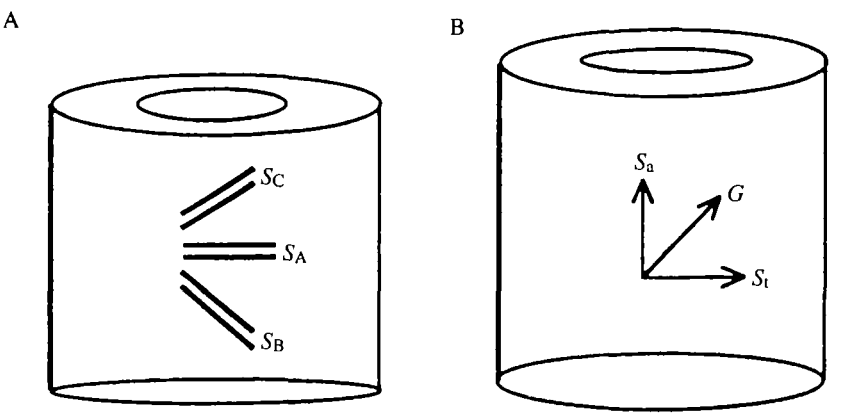

Fig. 1. Orientation of strain gauge elements (A) and calculated (Dally and Reilly, 1978) strains (B). Axial strain $(S_a)=[2(S_C+S_B)-S_A]/3$, transverse strain $(S_t)=S_A$ and shear strain $(G)=[(2\times3^{0.5})/3]\,(S_C+S_B)$, where S_a is axial strain, S_t is transverse strain and G is shear strain.

Results

Eleven exercise roosters ran a cumulative distance of 150 km during the 9-week exercise program; one exercise animal died of unknown causes in the third week. Distances increased by approximately 10 % per week, starting at 12.8 km the first week and finishing at 22.8 km by the ninth week. The average (±S.E.) age-matched control body mass (2.12±0.02 kg) significantly exceeded the basal control (1.89±0.02 kg) by 12 % and exercise (1.93±0.01 kg) body mass by 10 %.

Morphometry

No age- or exercise-related change in TMT length occurred, but an age-related increase in cortical cross section was measured, independent of exercise stimuli (Fig. 2). Changes in age-matched control cortical geometry could be accounted for by periosteal deposition and endosteal resorption, especially in the medial–lateral direction, with medial–lateral endosteal diameter increasing by 9 % compared to basal controls. In contrast, the exercise roosters deposited bone endosteally along the anterior–posterior plane, decreasing anterior–posterior endosteal diameter by 7 % compared to basal controls and significantly increasing anterior (8 %) and medial (20 %) cortical thicknesses (Fig. 3). Representative cross sections (Fig. 4) highlight group differences in cortical geometry.

Second moment of area about the bending (A_x) and nonbending (A_y) axes corresponded to the differences in regional cortical thickness and cortical area. Age-matched control A_x and A_y exceeded basal control values by 10 % and exercise values by 7 %, but neither difference was significant.

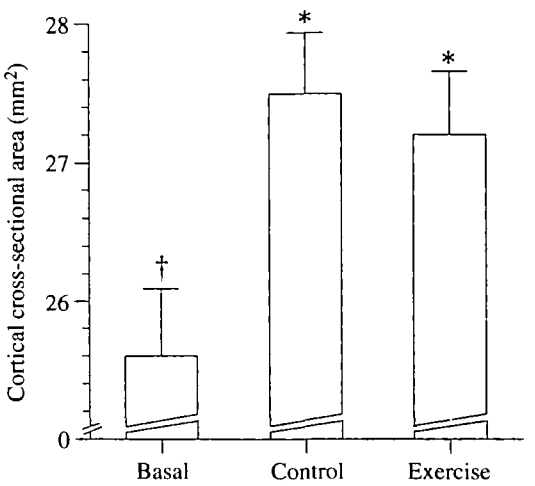

Fig. 2. Cortical cross-sectional areas of the basal control (Basal), age-matched control (Control) and exercise (Exercise) groups. Values are group means+S.E. Statistically significant ($P<0.05$) differences between groups are denoted with different symbols; values for groups with the same symbols are not statistically different.

Mechanical properties and density

Maximum load for the basal controls was significantly less than those for age-matched control (17 %) and exercise TMT (15 %) groups (Table 1). Failure loads also differed significantly between control groups (49 %); values for exercise group

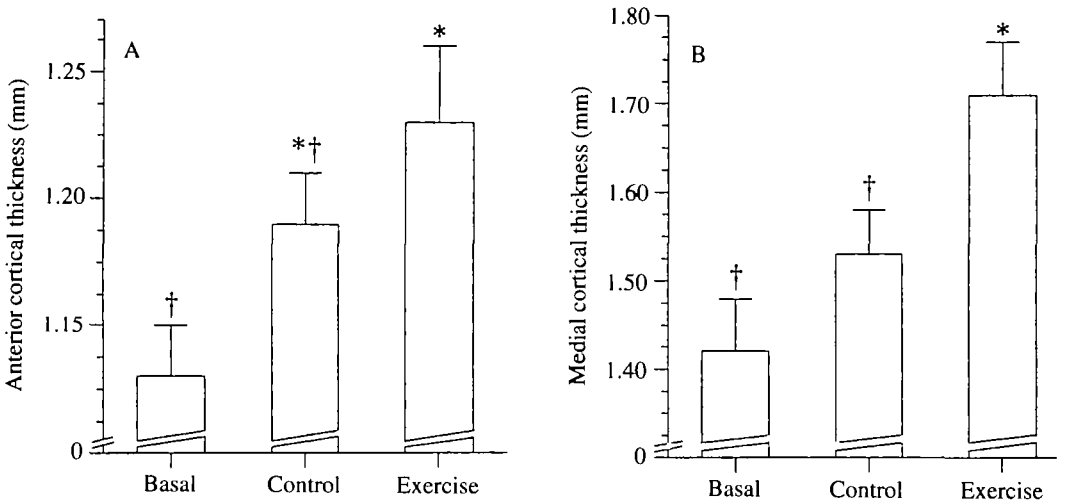

Fig. 3. Anterior (A) and medial (B) cortical thickness of the basal control (Basal), age-matched control (Control) and exercise (Exercise) groups. Values are group means+S.E. Statistically significant ($P<0.05$) differences between groups are denoted with different symbols; values for groups with the same symbols are not statistically different.

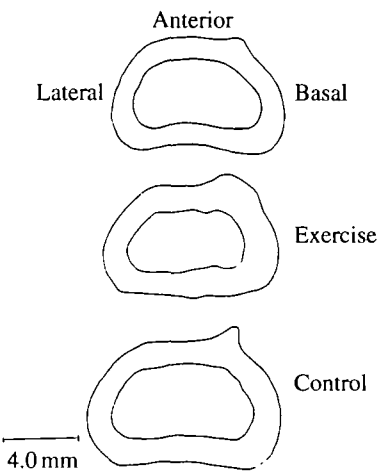

Fig. 4. Mid-diaphysial cross sections representative of the basal control, exercise and age-matched control tarsometatarsus geometry.

Table 1. *Structural and material properties of the tarsometatarsus*

	Basal control	Age-matched control	Exercise
Maximum load (N)	503.3±22.3*	590.9±13.3†	573.1±15.7†
Failure load (N)	290.6±38.0*	431.0±33.4†	376.4±33.9*†
Flexural rigidity ($kN\,mm^2$)	1.20±0.05	1.28±0.04	1.31±0.07
Elastic modulus (GPa)	13.2±0.7	12.7±0.5	13.9±0.9
Tensile stress at the proportional limit (MPa)	144.5±8.9	153.0±5.2	156.3±7.7
Density ($mg\,ml^{-1}$)	1.40±0.04*	1.58±0.01†	1.59±0.06†

Values are group means±S.E.; N=9 basal control, N=11 age-matched control, N=11 exercise. Statistically significant ($P<0.05$) differences between groups are denoted with different superscript symbols; in this table, (†) is significantly greater than (*).

failure loads lay between those of the control groups. Flexural rigidity did not differ among groups (Table 1).

No significant differences in material properties were detected among the groups (Table 1), although exercise elastic modulus exceeded the basal control value by 5 % and the age-matched control value by 9 %. Age-matched control and exercise tensile stress at the proportional limit exceeded the basal control value by 10 %. Age-matched control and exercise mid-diaphysial densities were similar, and both significantly exceeded the basal control value density (Table 1).

Gait kinematics

No significant differences in right/left stance durations occurred among the roosters of all groups. In age-matched controls (no surgical intervention), stance times varied by ±22 % from right to left. Comparable right–left symmetries occurred in animals following surgery, with no evidence that asymmetry resulted from surgical intervention or pain. Indeed, for two exercise animals implanted with strain gauges, at times the weightbearing duration on the surgical leg exceeded that on the nonsurgical leg by as much as 22 %.

In vivo *strains*

For the instrumented roosters (N=3 per group), strains were less than 65 microstrain during swing, but increased sharply during early stance. Shear strains tended to peak before midstance, while transverse and axial strains peaked at or after midstance (Fig. 5). Bimodal peaks occurred in 10 % of the trials, with single maximum peaks occurring in the remaining trials.

Significant differences in strain magnitudes were detected within groups. Roosters' strain profiles were similar across trials, except within the basal control group. Two basal control birds had similar medial and lateral strain magnitudes, but were substantially different from the third basal control bird; anterior strains

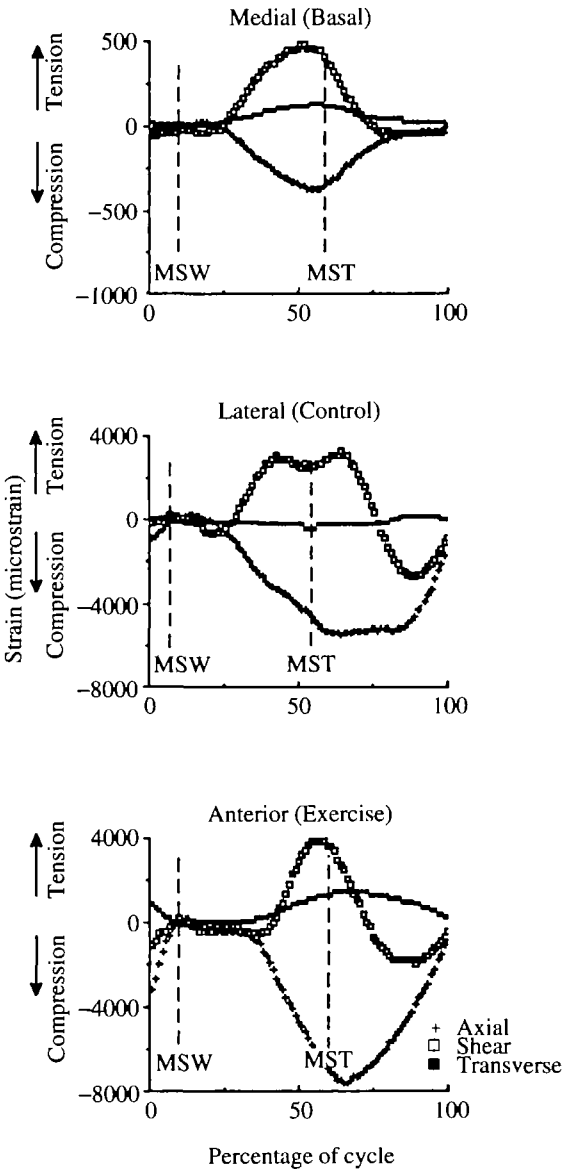

Fig. 5. Representative strains from each animal group for medial, lateral and anterior cortical surfaces. Percentage of gait cycle (right toe-off to right toe-off) is plotted along the abscissa; midswing (MSW) and midstance (MST) are indicated for each cycle. Strain (microstrain) is plotted on the ordinate; compression is negative and tension is positive. Strains were measured during slow walking ($37\,cm\,s^{-1}$).

differed among the three basal control birds. Nevertheless, even with the within-group variations, significant differences in strain magnitudes were found among groups.

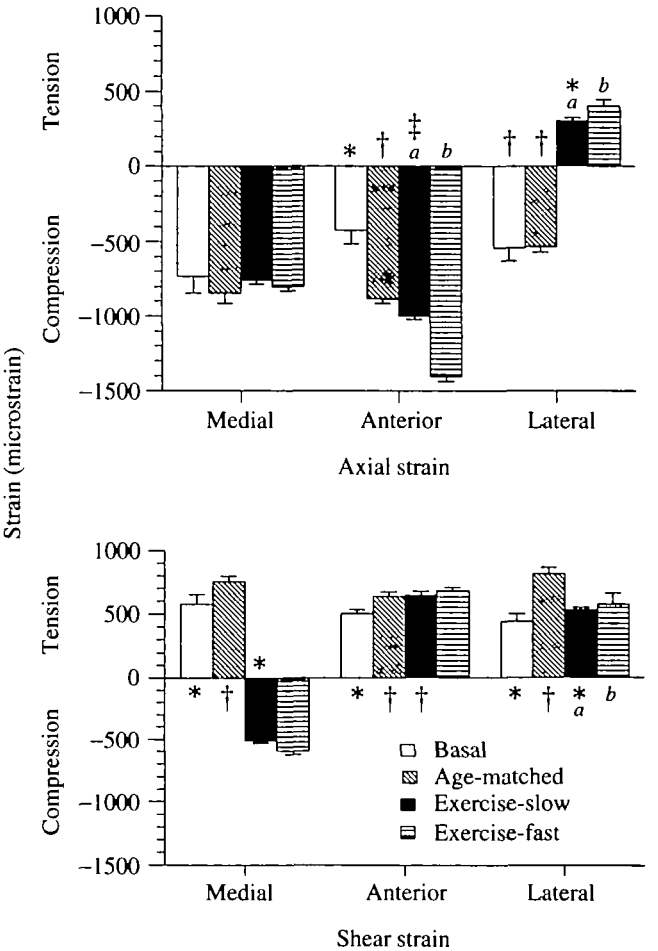

Fig. 6. Peak (mean+S.E.) axial and shear strains (microstrain) for medial, anterior and lateral tarsometatarsus surfaces during *slow* walking trials (37 cm s^{-1}) for basal, age-matched control and exercise groups (N=3 per group) and *fast* walking (87 cm s^{-1}) of the exercise group. For each bird, peak strains were averaged from 10 steps. Statistically significant (P<0.05) differences for the same cortical surface among basal, age-matched control and exercise groups (walking at the same slow speed) are denoted with differing symbols (*,†,‡), where ‡>†>*. Exercise-slow and Exercise-fast data are from the same exercised roosters walking at two different speeds. Statistically significant differences between these two groups are also denoted with differing superscripts (a,b), where b>a.

Slow walking

Compressive axial strains developed along the medial and anterior cortices for all groups (Fig. 6). Medially, no significant difference in axial strain magnitude (779±69 microstrain) occurred among groups. Peak anterior axial strain, however, differed significantly among groups, with the value for the exercise group

exceeding that of age-matched controls by 13% and that of basal controls by 136%; age-matched anterior axial strain exceeded basal strain by 123% (Fig. 6). Laterally, slight axial tension developed in the exercise group, while basal and age-matched control groups developed axial compression. Exercise axial strain (lateral surface) was significantly less than that of basal and age-matched controls (Fig. 6).

Shear strain differed widely within and among groups. Medially, basal controls and two age-matched controls developed tensile shear strain, while the remaining age-matched control and all exercise animals developed compressive shear strain (Fig. 6). Medial strain magnitude for age-matched controls significantly exceeded that of basal controls by 31% and that of exercise birds by 48%. Anteriorly, roosters experienced tensile shear strain, and basal strain was 26% less than that in exercise and age-matched controls (Fig. 6). Tensile shear also developed laterally. Strain magnitudes of the age-matched control group significantly exceeded values in the basal control and exercise groups.

No significant differences in transverse strain magnitude were found among groups, with transverse strains tending to be smaller than axial and shear strains. Anterior and medial surfaces strained in tension, while all TMTs experienced transverse compression laterally (Fig. 5).

Fast walking

Axial strain patterns were similar between the slow- and fast-walking trials examined for the exercise group (Fig. 6), but magnitude increased laterally by 31% and anteriorly by 40% during fast (54% of maximum training speed) walking; medial axial strain magnitude did not change. Shear strain patterns were irregular during fast walking, with greater individual differences noted among birds. Anterior and medial shear strain magnitudes were similar between fast- and slow-walking groups, and lateral surface shear strain increased by 9% at the faster speed. Transverse strain magnitude increased medially (44%) and decreased laterally (16%) at the faster speed. The magnitude of the anterior surface transverse strain was not affected by walking speed.

Discussion

The current study has quantified the exercise-induced changes of mature bone. While reports have described various interactive effects of growth and exercise on bone remodelling (Biewener *et al.* 1986; Matsuda *et al.* 1986), no study has described the *in vivo* effects of strenuous exercise on adult bone. Several earlier studies have examined the effects of altered loading through invasive transcortical pins (Rubin and Lanyon, 1984, 1985) or unilateral radial or ulnar excision (Carter *et al.* 1980; Goodship *et al.* 1979; Lanyon *et al.* 1982), but here loads were increased with an activity within the animal's physiological repertoire.

Although consistent with age-related changes previously reported (Harvey *et al.* 1979; Latimer, 1927), the differences in TMT geometry and animal mass between

basal and age-matched controls highlighted difficulties in defining skeletal maturity. In terms of longitudinal growth, the roosters were mature; closed physes prevented increased bone length. Latimer (1927) characterized bone growth in White Leghorn roosters from hatching to 300 days. TMT growth ceased after 142 days, and average bone length was 102.2 mm. Similarly, the 3–4 % per week increase in our age-matched control mass was consistent with previous reports of typical mass changes (Harvey *et al.* 1979). These data suggest that the periosteal deposition and endosteal resorption that led to the increased cortical thickness and cross-sectional area may be attributable to the continued increase in animal mass rather than to growth-related processes. The 30-week-old roosters in the present study were neither senescent nor skeletally 'immature', and a more thorough analysis of the effects of increased animal mass on rooster skeletal geometry after physial closure should be a topic for further study.

Regardless of the definition of skeletal maturity, strenuous exercise altered normal age-related bone remodelling by stimulating bone deposition endosteally rather than periosteally. Similar exercise-related geometry changes have been reported in immature roosters (Matsuda *et al.* 1986) and immature swine (Woo *et al.* 1981). Our current data on adult roosters and those of Matsuda *et al.* (1986) on growing roosters suggest site-specific deposition for each age group in response to the dynamics of the strenuous exercise; bone was deposited anteromedially in adult birds and anterolaterally in growing animals. Kinematic and dynamic analyses of growing and adult rooster will be needed to help explain these site-specific changes in TMTs.

Conflicting findings about exercise-related changes in bone mechanical properties (Keller and Spengler, 1989; Matsuda *et al.* 1986; Rubin and Lanyon, 1984) may reflect complex interactions between bone remodelling and exercise intensity, animal species and skeletal age. Woo *et al.* (1981) attributed exercise-related increases in bone structural properties to greater cortical cross-sectional area. A similar conclusion cannot be drawn from our data, because TMT maximum load and cortical area did not differ between the exercise and age-matched control groups. Thus, unlike rapidly growing chicks (Matsuda *et al.* 1986), strenuous running in adult roosters redistributed bone mass while maintaining cortical area, and did not alter normal, age-related bone mechanical properties.

Strain magnitudes reported here are similar to those previously reported (Biewener *et al.* 1986; Keller and Spengler, 1989; Rubin and Lanyon, 1985). Strains greater than 1000 microstrain can stimulate adaptive remodelling in the turkey ulna (Rubin and Lanyon, 1985), whereas strains greater than 5000 microstrain have been associated with increased fracture risk in racehorses (Nunamaker *et al.* 1987). *In vivo* strain data during fast walking (87 cm s^{-1}) in the present study were collected at a speed 46 % slower than the speed at which the roosters trained at the end of the exercise protocol. Therefore, the strains during the daily exercise bouts were probably greater than the 1000 microstrain magnitude suggested as an 'osteogenic' threshold, but less than that associated with increased fracture incidence.

Differences between basal and age-matched control strains suggest that the optimal strain state maintained by a bone changes with age. This is at variance with the hypothesis that bone remodelling is driven by the need to maintain similar surface strains (Biewener *et al.* 1986; Goodship *et al.* 1979; Keller and Spengler, 1989; Rubin and Lanyon, 1984). Biewener *et al.* (1986) reported comparable strains in the chick tibia during 12 weeks of rapid growth marked by a threefold increase in bone length. Lanyon *et al.* (1982) report similar data for mature sheep; following ulnar osteotomy, the radius was remodelled until mid-shaft strains returned to preoperative levels, suggesting that strain directed remodelling until an accustomed strain state was achieved. The significantly greater strains in our age-matched controls indicate that this may not be the case for the avian skeleton after epiphysial closure and cessation of longitudinal bone growth. Our findings may reflect the increased animal mass in the age-matched controls compared to that of the basal control roosters. Increased animal mass resulted in greater mid-diaphysial deflection and surface strains and the stimulation of periosteal bone deposition. The disparity in these different studies may highlight differences between the immature and mature skeleton and, taken together, the data suggest that the role of strain as a remodelling stimulus may be different in immature and mature bone.

Our exercise strain data apparently contradict Biewener *et al.* (1986) and Keller and Spengler (1989), who state that strain remains constant despite exercise stimuli. Differences in experimental design may account for these apparent contradictions because both earlier studies used exercise considerably less strenuous than we used. Lanyon (1987) suggests that a bone's ability to detect strain relies on gradients of strain-related stimuli between surface osteocytes and osteoblasts. If the strain distribution experienced by surface cells falls within a certain range, no remodelling response occurs, but if a mismatch develops between a cell's accustomed state and the current strain state, then remodelling results. In previous exercise studies, strains experienced during exercise may not have exceeded the threshold to stimulate surface cells.

Currey (1984) and Currey and Alexander (1985) predict that, to provide mechanical support, a bone must maintain a certain stiffness and strength, while minimizing mass and energy expenditure during movement. By expressing cortical geometry as the ratio of periosteal radius (rad) to wall thickness (t), Currey and Alexander (1985) quantified the mass saved by a marrow-filled bone with a tubular configuration rather than a solid block, while maintaining similar structural properties. For example, for two bones with the same stiffness, a rad/t value of 4.2 results in a 17 % mass reduction for the tubular bone compared to the solid bone. By calculating rad/t values for specific cortical surfaces, one can compare the mass savings for the marrow-filled, tubular TMT compared to those of a solid bone and predict the structural property maintained during remodelling.

Our basal and age-matched controls and exercise rad/t values suggest that exercise-induced remodelling tended to maintain ultimate or impact strength for the medial, anterior and posterior cortices. Our experimental data and the

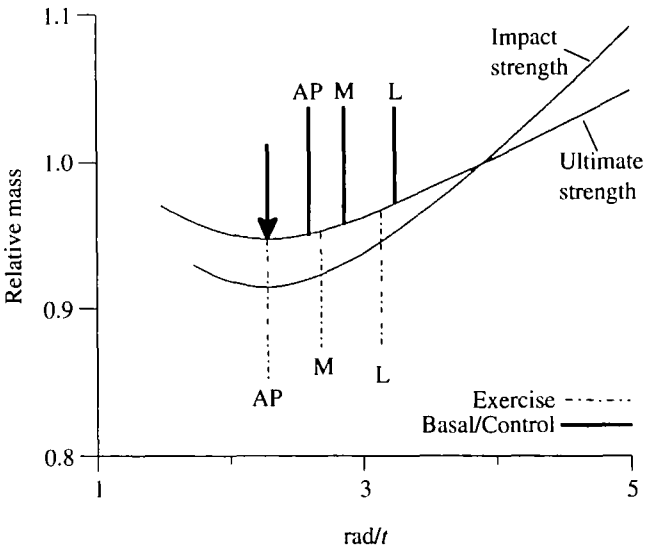

Fig. 7. Cortical geometry, expressed as rad/t, from the present study are superimposed on the theoretical curves adapted from Currey and Alexander (1985). The ratio rad/t of periosteal radius (rad) to wall thickness (t) is plotted on the abscissa; the ordinate is the mass of marrow-filled tubular bone compared to the mass of a solid bone with the same mechanical property (ultimate or impact strength). The experimental rad/t values of basal and age-matched controls (Basal/Control) cortical regions intercept the theoretical curve as solid lines; exercise rad/t values are plotted as dashed lines. The arrow represents Currey and Alexander's predicted rad/t value (2.3) that minimizes mass while optimizing bone ultimate or impact strength. Cortical regions are abbreviated as M (medial), L (lateral) and AP (anterior and posterior). (Medial exercise rad/t is significantly less than medial basal/control rad/t, $P<0.05$.)

Currey–Alexander theoretical curves for impact and ultimate strength are shown in Fig. 7. For all cortical surfaces, exercise rad/t values were less than control and basal values, with the medial rad/t significantly less than age-matched and basal control values. These theoretical data distinguish exercise TMTs from basal and age-matched control TMTs and are consistent with the elevated maximum load (ultimate strength) in the exercise TMTs. We did not test TMT impact strength; therefore, we cannot say how changes in TMT geometry might have influenced impact strength. These data may help to explain the exercise-related endosteal deposition and suggest that, while minimizing bone mass, the structural property optimized during exercise-induced remodelling may differ from that optimized during typical, age-related remodelling. Interestingly, published radius cortical thickness data (Matsuda *et al.* 1986) for strenuously exercised immature roosters also support the Currey and Alexander predictions; exercise rad/t values were

consistently smaller than values for sedentary controls, except for the medial TMT cortex.

Was bone mass conserved during age- and exercise-related remodelling? For a column loaded in bending, mass is related to density (D) and elastic modulus (E) as $D/E^{0.5}$ (Currey, 1984). For our data, we can predict changes in bone mass by the concomitant changes in bone density and elastic modulus. This calculation reveals that bone mass did not differ significantly among groups; that is, despite an age-related increase in bone density, concomitant changes in bone distribution resulted in off-setting changes in elastic modulus while bone mass was maintained. This suggests that conservation of bone mass is important in age-related bone remodelling. In addition, energy expenditure may be a potent constraint when endurance exercise is the overload stimulus for bone remodelling. In roosters, running speed and energy expenditure are linearly correlated (Brackenbury and Avery, 1980) and energy conservation is an important objective for the exercising birds. Maintaining bone mass may be particularly important for a more distal bone (TMT) because an increased moment of inertia would require greater proximal muscle forces to move the limb. During exercise, the remodelling response stimulated by increased strains may be influenced by the objective of maintaining bone mass while maximizing ultimate strength – with the resulting bone shape being a compromise between mechanical and physiological objectives.

The authors thank Ben Croy for technical assistance with the strain gauge amplifiers, Klaus Schneider for computer programming and the anonymous manuscript referees for valuable feedback on our data analyses and interpretations. This study was supported in part by the Dorothy and Leonard Strauss Sports Medicine Fund and the California Physical Therapy Fund (no. 88-10).

References

Biewener, A. A., Swartz, S. M. and Bertram, J. E. (1986). Bone modeling during growth: Dynamic strain equilibrium in the chick tibiotarsus. *Calcif. Tissue Int.* **39**, 390–395.

Brackenbury, J. H. and Avery, P. (1980). Energy consumption and ventilatory mechanisms in exercising fowl. *Comp. Biochem. Physiol.* **66**A, 439–445.

Carter, D. R., Smith, D. J., Spengler, D. M., Daly, C. H. and Frankel, V. H. (1980). Measurement and analysis of *in vivo* bone strains on the canine radius and ulna. *J. Biomech.* **13**, 27–38.

Cowin, S. C., Lanyon, L. E. and Rodan, G. (1984). The Kroc Foundation conference on functional adaptation in bone tissue. *Calcif. Tissue Int.* **36**, S1–S6.

Currey, J. D. (1984). *The Mechanical Adaptations of Bones*, pp. 98–126. Princeton, New Jersey: Princeton University Press.

Currey, J. D. and Alexander, R. McN. (1985). The thickness of the walls of tubular bones. *J. Zool., Lond.* **206**, 453–468.

Dalen, N. and Olsson, K. E. (1974). Bone mineral content and physical activity. *Acta orthop. scand.* **45**, 170–174.

Dally, J. W. and Reilly, W. F. (1978). *Experimental Stress Analysis*. pp. 18–327. New York: McGraw Hill.

Goodship, A. E., Lanyon, L. E. and Macfie, H. (1979). Functional adaptation of bone to increased stress. *J. Bone Joint Surg.* **61**A, 539–546.

Harvey, S., Scanes, C. G., Chadwick, A. and Bolton, N. J. (1979). Growth hormone and

prolactin secretion in growing domestic fowl: Influences of sex and breed. *Br. Poult. Sci.* **20**, 9–17.

JONES, H. H., PRIEST, B., HAYES, W. C., TICHENOR, C. C. AND NAGEL, A. (1977). Humeral hypertrophy in response to exercise. *J. Bone Joint Surg.* **59**A, 204–208.

KELLER, T. S. AND SPENGLER, D. M. (1989). Regulation of bone stress and strain in the immature and mature rat femur. *J. Biomech.* **22**, 1115–1128.

KIISKINEN, A. (1977). Physical training and connective tissues in young mice-physical properties of achilles tendons and long bones. *Growth* **41**, 123–137.

KROLNER, B., TOFT, B., NIELSON, S. P. AND TONDEVOLD, E. (1983). Physical exercise as prophylaxis against involutional vertebral bone loss: A controlled trial. *Clin. Sci.* **64**, 541–546.

LANYON, L. E. (1987). Functional strain in bone tissue as an objective and controlling stimulus for adaptive bone remodelling. *J. Biomech.* **20**, 1083–1093.

LANYON, L. E., GOODSHIP, A. E., PYE, C. J. AND MACFIE, H. (1982). Mechanically adaptive bone remodelling. A quantitative study of functional adaptation in the radius following ulnar osteotomy in sheep. *J. Biomech.* **15**, 141–154.

LATIMER, H. B. (1927). Postnatal growth of the chicken skeleton. *Am. J. Anat.* **40**, 1–57.

MATSUDA, J. J., ZERNICKE, R. F., VAILAS, A. C., PEDRINI, V. A., PEDRINI-MILLE, A. AND MAYNARD, J. A. (1986). Structural and mechanical adaptation of immature bone to strenuous exercise. *J. appl. Physiol.* **60**, 2028–2034.

NAGURKA, M. L. AND HAYES, W. C. (1980). An interactive graphics package for calculating cross sectional properties of complex shapes. *J. Biomech.* **13**, 59–64.

NUNAMAKER, D. M., BUTTERWICK, D. M. AND BLACK, J. (1987). Fatigue fracture in racehorses: Relationships with age and strain. *Trans. orthop. Res. Soc.* **12**, 72.

PIRNAY, F., BODEUX, M., CRIELAARD, J. M. AND FRANCHIMONT, P. (1987). Bone mineral content and physical activity. *Int. J. Sports Med.* **8**, 331–335.

RUBIN, C. T. (1984). Skeletal strain and the functional significance of bone architecture. *Calcif. Tissue Int.* **36**, S11-S18.

RUBIN, C. T. AND LANYON, L. E. (1984). Regulation of bone formation by applied dynamic loads. *J. Bone Joint Surg.* **66**A, 397–402.

RUBIN, C. T. AND LANYON, L. E. (1985). Regulation of bone mass by mechanical strain magnitude. *Calcif. Tissue Int.* **37**, 411–417.

TORZILLI, P. A., TAKEBE, K., BURSTEIN, A. H. AND HEIPLE, K. G. (1981). Structural properties of immature canine bone. *Trans. ASME* **103**, 232–238.

WOO, S. L.-Y., KUEI, S. C., AMIEL, D., GOMEZ, M. A., HAYES, W. C., WHITE, F. C. AND AKESON, W. H. (1981). The effect of physical training on the properties of long bone: A study of Wolff's law. *J. Bone Joint Surg.* **63**A, 780–787.